JACS
JOURNAL OF THE AMERICAN CHEMICAL SOCIETY

Article

pubs.acs.org/JACS

Mechanism of the Electrocatalytic Reduction of Protons with Diaryldithiolene Cobalt Complexes

Christopher S. Letko,[†] Julien A. Panetier,[†] Martin Head-Gordon,*[,‡] and T. Don Tilley*[,‡]

Joint Center for Artificial Photosynthesis, [†]Materials Sciences Division and [‡]Chemical Sciences Division, Lawrence Berkeley National Laboratory, University of California, Berkeley, California 94720, United States

Supporting Information

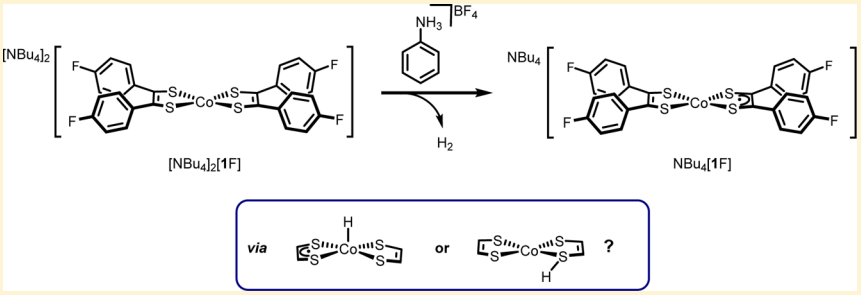

ABSTRACT: A series of dimeric cobalt-diaryldithiolene complexes $[Co(S_2C_2Ar_2)_2]_2$, possessing various aryl *para* substituents (OMe, F, Cl, and Br), were studied as electrocatalysts for proton reduction in nonaqueous media, in an effort to correlate dithiolene donor strength with catalyst activity. Cyclic voltammetry data acquired for the cobalt-diaryldithiolene dimers guided the isolation of chemically reduced monoanionic ($[Co(S_2C_2Ar_2)_2]^-$) and dianionic ($[Co(S_2C_2Ar_2)_2]^{2-}$) monomers. The potassium and tetrabutylammonium salts of dianionic cobalt-diaryldithiolene complexes have been characterized by single crystal X-ray crystallography. Treatment of the dianionic species with stoichiometric quantities of a weak acid afforded H_2 and the monoanionic cobalt-diaryldithiolene species. Density functional theory (BP86) suggests that hydrogen elimination proceeds through a diprotonated intermediate with a Co−H bond and a protonated S center. A transition state for transfer of the S−H proton to the metal center was located with a computed free energy of 5.9 kcal/mol, in solution (DMF via C-PCM approach).

INTRODUCTION

The growing interest in renewable energy has focused considerable attention on artificial photosynthesis for the conversion of solar energy to chemical fuel.[1] One of the significant challenges in the development of this technology concerns the requirement that a scalable solar-fuels device be constructed from earth-abundant components. Thus, viable catalysts to be utilized for more efficient energy conversions and the minimization of overpotentials associated with the energy-storing reactions are based on first-row transition metals. Effective molecular electrocatalysts for the cathodic, hydrogen-evolving reaction (HER)[2] have been identified, including Co-glyoxime[3−6] and Co-tetraazamacrocycle[7] complexes, derivatives of $[Ni(P^R_2N^{R'}_2)_2]^{2+}$[8−10] and $[Co(bdt)_2]^-$ (bdt = 1,2-benzenedithiolate) complexes[11,12] (Figure 1). Considerable research over the past 10 years has focused on enhancing the activities and stabilities of such catalysts.[13]

The design and optimization of HER catalysts critically relies on a detailed understanding of the fundamental mechanistic steps involved in the conversion of protons and electrons to dihydrogen.[14,15] Commonly proposed mechanisms for HER electrocatalysts invoke an intermediate M−H species that is reduced to increase its basicity, and then protonation of this reduced M−H intermediate results in a direct precursor to H_2 elimination. These transformations suggest possible catalyst design elements that might be used to achieve more efficient catalysis. For example, the incorporation of non-innocent ligands to store reducing equivalents in the catalytic complex can lower the required potential to facilitate charge transfer, as has been suggested for Ni-glyoxime systems.[16] Additionally, catalysts may be modified to promote a protonation step, as has been achieved by DuBois and co-workers by incorporation of a pendent proton relay (Figure 1c).[8−10]

Dithiolene ligands[17−20] incorporate two fundamental properties that are potentially useful in the design of HER electrocatalysts. First, their redox-active nature should allow for the storage of reducing equivalents, and second, the sulfur donor atoms may serve as proton relays. The potential utility of such catalysts is indicated by recent studies by Eisenberg and Holland on derivatives of $[Co(bdt)_2]^-$ (bdt = 1,2-benzenedithiolate) as photocatalysts and electrocatalysts for proton reduction.[11,12,21] Their cyclic voltammetry (CV) studies support an ECEC mechanism for catalysis, in which the reduced $[Co(bdt)_2]^{2-}$ species is protonated, and subsequent reduction and protonation steps yield H_2 and regenerate $[Co(bdt)_2]^-$. However, experimental studies involving the proposed intermediates have yet to be reported.

Received: March 3, 2014
Published: June 20, 2014

   dx.doi.org/10.1021/ja5019755 | J. Am. Chem. Soc. 2014, 136, 9364−9376

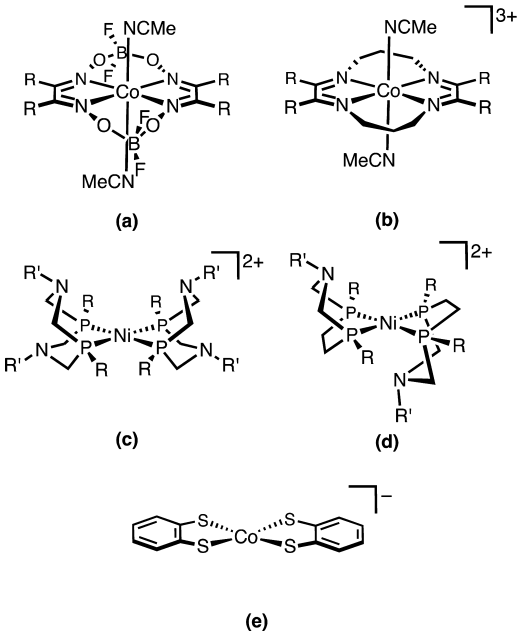

Figure 1. Selected general structures of first-row transition metal complexes demonstrated to be active proton reduction electrocatalysts: (a) Co-diglyoxime; (b) Co-tetraazamacrocycle; (c) $[Ni(P^R_2N^{R'}_2)_2]^{2+}$; (d) $[Ni(P^R_2N^{R'})_2]^{2+}$; (e) $[Co(bdt)_2]^-$.

Homoleptic Co-diaryldithiolene complexes have not been evaluated for electrocatalytic proton reduction activity, although the parent Co-diphenyldithiolene complex was first isolated by Schrauzer and co-workers in 1966.[22] Cobalt-bis(diaryldithiolene)s formally exist as neutral, Co−S bridged dimers in the ground state. The monomeric units are Lewis acidic and coordinate a variety of phosphines and phosphites at Co to afford neutral, monomeric adducts of the type $[Co(L)(S_2C_2Ph_2)_2]$ (L = phosphine, phosphite).[23] Phosphine adducts of this type can be electrochemically reduced to cleave the Co-phosphine bond, with generation of the anionic monomer, $[Co(S_2C_2Ph_2)_2]^-$.[24]

The electronic properties of diaryldithiolene ligands may be varied via substituents on the aryl rings, to allow tuning of both the redox properties of the metal center and the basicity of the S atoms. In a related study, DuBois and co-workers demonstrated that decreasing the basicity of pendent amines in $[Ni(P^{Ph}_2N^{R'}_2)_2]^{2+}$ (R′ = aryl) complexes affords a remarkable increase in proton reduction activity.[9] These studies revealed that decreasing the electron-donating character of the N-R′ substituents (Figure 1c) resulted in lower overpotentials by inductively shifting the Ni(II/I) and Ni(I/0) redox couples to more positive potentials. This change in structure also facilitates proton transfer from the less basic N atoms to the Ni center, which appears to also contribute to an increased rate for proton reduction. In addition, recent calculations by the Hammes-Schiffer group suggest that S atom basicity plays a key role in the catalytic activity of $[Co(bdt)_2]^-$ derivatives, such that protonation at sulfur inductively shifts the catalytic event to more positive potentials.[25] In this case, the calculations were performed using the B3P86 functional, which was found to be in agreement with the triplet ground states found experimentally for $[Co(bdt)_2]^-$, $[Co(tdt)_2]^-$, and $[Co(Cl_2bdt)_2]^-$.[11,26,27]

Density functional theory (DFT) calculations have played a significant role in providing an understanding of the electronic structures of cobalt-bis(dithiolene) species.[25,28−33] Neese, Wieghardt, and co-workers studied the monoanionic complex $\{Co[S_2(3,5\text{-}^tBu_2C_6H_2)]_2\}^-$.[29] Unrestricted B3LYP calculations suggested that the ground state of the benzene dithiolate complex $\{Co[S_2(3,5\text{-}^tBu_2C_6H_2)]_2\}^-$ is a triplet in which the Co $3d_{xy}$ orbital is isoenergetic with the highest π^*-b_{2g} system of the ligand. This implies that the monoanionic complex $\{Co[S_2(3,5\text{-}^tBu_2C_6H_2)]_2\}^-$ may have both Co(II) and Co(III) character, as observed for $[Co(bdt)_2]^-$. The choice of the DFT functional is another challenge in probing the ground state of these cobalt-bis(dithiolene) species. Wang et al.[33] performed DFT (BP86, pure-GGA) calculations on $[Co(mnt)_2]^-$ (mnt = $S_2C_2(CN)_2$) and predicted that singlet and triplet states are degenerate while DFT (B3P86, Hybrid-GGA) calculations of Solis and Hammes-Schiffer favored the triplet ground state.[25]

This report describes an experimental and theoretical investigation of electrocatalytic proton reduction by a series of Co-diaryldithiolene derivatives. These derivatives differ by the nature of the aryl *para* substituents, which were expected to tune the basicity of the S atoms. Reduced intermediates relevant to the catalytic cycle were isolated and probed in stoichiometric reactions with protons, which in combination with DFT calculations has allowed for construction of a likely mechanism for catalysis.

RESULTS AND DISCUSSION

Synthesis and Electrochemistry of Cobalt-Diaryldithiolene Dimers. Neutral, dimeric dithiolene complexes of cobalt were synthesized following a modified version of a procedure published by Schrauzer and co-workers.[22] In general, a 4,4′-substituted benzil was thionated with phosphorus pentasulfide to generate a thiophosphate intermediate, which was then treated with an aqueous solution of cobalt(II) chloride to afford the dimeric, dithiolene complexes $[\mathbf{1}X]_2$ (X = F, Cl, Br; eq 1).[34,35] The complex $[\mathbf{1}OMe]_2$ was reported

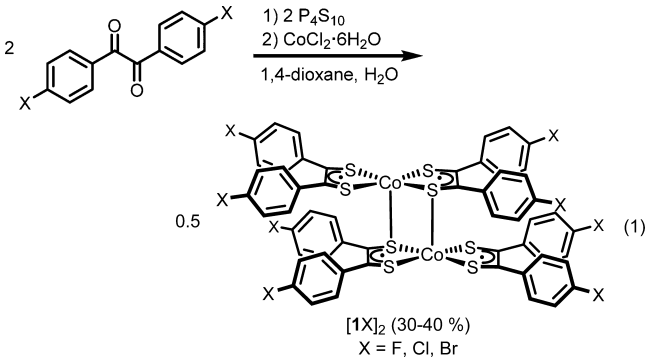

(1)

previously.[24] This method, which reliably gave yields of 30−40%, is convenient given the commercial availability of many benzil starting materials. The 4,4′-dichlorobenzil starting material was synthesized via a McMurry coupling[36] of *p*-chlorobenzaldehyde to afford 1,2-bis(4-chlorophenyl)ethane-1,2-diol as a mixture of diastereomers, followed by oxidation of the vicinal diol using 2-iodoxybenzoic acid (IBX).[37] The X substituents span a broad range of *para*-substituent Hammett parameters, with σ values of −0.268 (OMe), +0.062 (F), +0.227 (Cl), and +0.232 (Br).[38] Attempts to extend this methodology to cyano and trifluoromethyl derivatives have so far been unsuccessful, presumably because the corresponding, more electrophilic benzil derivatives are unreactive toward phosphorus pentasulfide.[35]

dx.doi.org/10.1021/ja5019755 | J. Am. Chem. Soc. 2014, 136, 9364−9376

The bromine derivative $[\mathbf{1}Br]_2$ was characterized by single crystal X-ray diffraction (Figure 2). The bis(dithiolene)

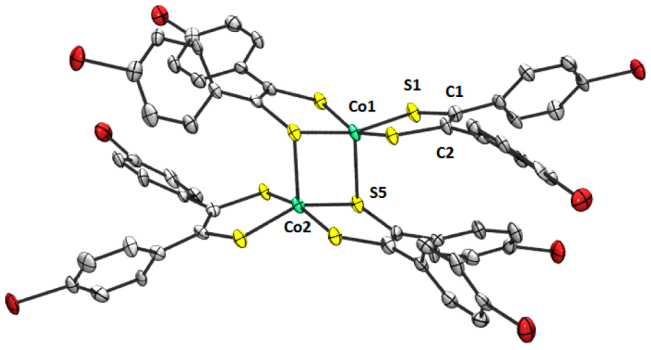

Figure 2. Molecular structure of $[\mathbf{1}Br]_2$ with thermal ellipsoids displayed at a 50% probability level. Hydrogen atoms have been omitted for clarity.

monomeric units are associated through apical coordination of a ligand S atom to a neighboring Co center, to give an approximate square pyramidal coordination geometry. In general, this structure exhibits metric parameters that coincide well with reported data for $[\mathbf{1}OMe]_2$.[24] The C1−C2 bond distance of 1.41(2) Å is longer than that of an ideal C−C double bond, which is characteristic of the radical anion oxidation state of the ligand. The $[\mathbf{1}X]_2$ complexes exist in the ground state as neutral, diamagnetic dimers, and on the basis of studies of analogous dimeric Fe-diaryldithiolene complexes,[39] this appears to result from antiferromagnetic coupling between the unpaired electrons.

Cyclic voltammetry (CV) data for $[\mathbf{1}F]_2$, $[\mathbf{1}Cl]_2$, $[\mathbf{1}Br]_2$, and $[\mathbf{1}OMe]_2$ are similar to that reported for $[Co(S_2C_2(CF_3)_2)_2]_2$ (Figure 3).[40] The solvent used for CV measurements was DMF, since the neutral dimers are insoluble in MeCN. Three reduction events are observed in each case, and the corresponding reduction potentials correlate linearly with the Hammett parameters for the X substituents. The final reduction event for these complexes spans ca. 200 mV between the $[\mathbf{1}OMe]_2$ and $[\mathbf{1}Cl]_2$ derivatives. The first redox wave (A in

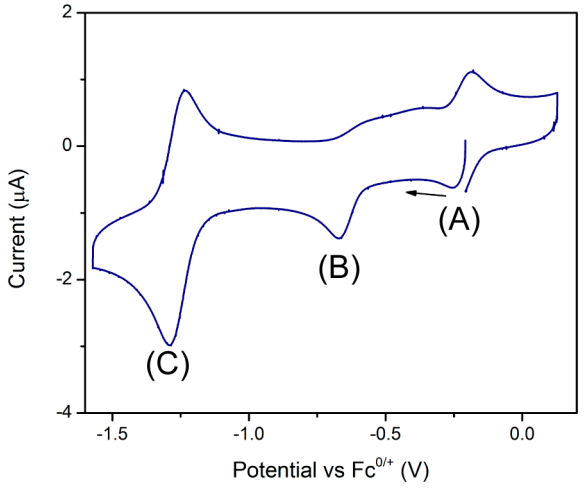

Figure 3. Cyclic voltammogram for $[\mathbf{1}Br]_2$ (0.15 mM) in DMF solution with 0.1 M $[NBu_4]PF_6$ as the supporting electrolyte. The labeled redox events correspond to the similarly denoted steps in Scheme 1.

Figure 3) is reversible and corresponds to reduction of dimeric units by one electron, to $[\mathbf{1}X]_2^-$ (Scheme 1). This is followed by a second, irreversible one-electron event to afford $[\mathbf{1}X]_2^{2-}$ (Scheme 1, Step B). Donahue and co-workers have structurally characterized $[NEt_4]_2[\mathbf{1}OMe]_2$ and $[NBu_4][\mathbf{1}OMe]$, which suggests that these two species are stable and could exist in equilibrium (K_D, Scheme 1).[24] Thus, the irreversible reduction event corresponding to the formation of $[\mathbf{1}X]_2^{2-}$ could be attributed to the chemical conversion of monomeric $[\mathbf{1}X]^-$ to $[\mathbf{1}X]_2^{2-}$ by this equilibrium. The monomeric, anionic species $[\mathbf{1}X]^-$ can accept an additional electron to form a dianion, $[\mathbf{1}X]^{2-}$, which is reversible in each case (e.g., for X = Br, i_{pc}/i_{pa} = 0.9). The current density associated with this $[\mathbf{1}X]^-/[\mathbf{1}X]^{2-}$ reduction event is twice that of the preceding one-electron events and is characterized by a peak separation of greater than 60 mV for all derivatives (e.g., for X = Br, ΔE_p = 80 mV). Thus, this reduction process corresponds to the one-electron reduction of two monomeric units ($2e^-$/dimer).[40,41] Table 1 compares the reduction potentials for the four derivatives examined (all potentials herein are referenced internally to ferrocene, Fc).

Electrocatalytic Proton Reduction Studies. Addition of anilinium tetrafluoroborate ($AnBF_4$, pK_a = 4.3 in DMF) to a DMF solution of $[\mathbf{1}Br]_2$ resulted in observation of a catalytic current at E_{pc} = −1.45 V. Catalytic proton reduction by $[\mathbf{1}Br]_2$ is observed at a modest overpotential of 350 mV at the catalytic current half-peak height ($E_{p/2}$; E°_{AnBF4} in DMF = −0.99 V;[42] Figure 4, top). The Faradaic yield associated with this electrocatalysis, determined by bulk electrolysis combined with gas chromatographic monitoring of H_2 formation, was 90 ± 10% (at −1.47 V). Observation of a catalytic wave just negative to the $[\mathbf{1}Br]^-/[\mathbf{1}Br]^{2-}$ wave ($E_{1/2}$ = −1.27 V) suggests a mechanism that is more complicated than EC′. An EC′ mechanism for proton reduction would likely proceed via double protonation of $[\mathbf{1}Br]^{2-}$, followed by subsequent release of H_2, and would be reflected by a growth in catalytic current at the $[\mathbf{1}Br]^-/[\mathbf{1}Br]^{2-}$ redox wave. Instead, a likely pathway involves initial protonation of $[\mathbf{1}Br]^{2-}$, followed by reduction of this protonated species before a second protonation event occurs to liberate H_2 (an ECEC mechanism as shown in Scheme 2). Although Co-dithiolene complexes have been demonstrated to bind amine and phosphine Lewis bases,[23,43−45] CV features of $[\mathbf{1}Br]_2$ were not perturbed upon addition of 130 equiv of the conjugate base, aniline (Figure S3 in Supporting Information). The catalytic behavior of $[\mathbf{1}Cl]_2$ was found to be identical to that of $[\mathbf{1}Br]_2$ (Figure S4 in Supporting Information).

The fluoro and methoxy derivatives also exhibit catalytic currents in the presence of $AnBF_4$ (Figure 4, middle and bottom), with $E_{p/2}$ values of −1.37 V and −1.46 V, respectively ($NBu_4[\mathbf{1}F]$ was studied due to the poor solubility of $[\mathbf{1}F]_2$ in DMF). In these cases, there is a smaller difference between $E_{p/2}$ values, as compared to those for the $[\mathbf{1}X]^-/[\mathbf{1}X]^{2-}$ couples (ca. −0.040 V for $NBu_4[\mathbf{1}F]$ and −0.080 V for $[\mathbf{1}OMe]_2$). Given this behavior, a similar ECEC mechanism is presumed to be operative.

Dichloroacetic acid (DCA, pK_a = 7.2 in DMF),[46] a weaker acid than $AnBF_4$, was also employed to probe the catalytic behavior of $[\mathbf{1}Br]_2$ and $[\mathbf{1}OMe]_2$. The reduction of $[\mathbf{1}Br]_2$ to $[\mathbf{1}Br]^{2-}$ in the presence of 130 equiv of DCA (DMF solution) did not result in the observation of a catalytic current. Under the same conditions, $[\mathbf{1}OMe]_2$ was found to exhibit a catalytic current, and $E_{p/2}$ was observed to shift by −0.060 V with

dx.doi.org/10.1021/ja5019755 | J. Am. Chem. Soc. 2014, 136, 9364−9376

Scheme 1. Sequence of Reduction Events for Cobalt-diaryldithiolene Derivatives[a]

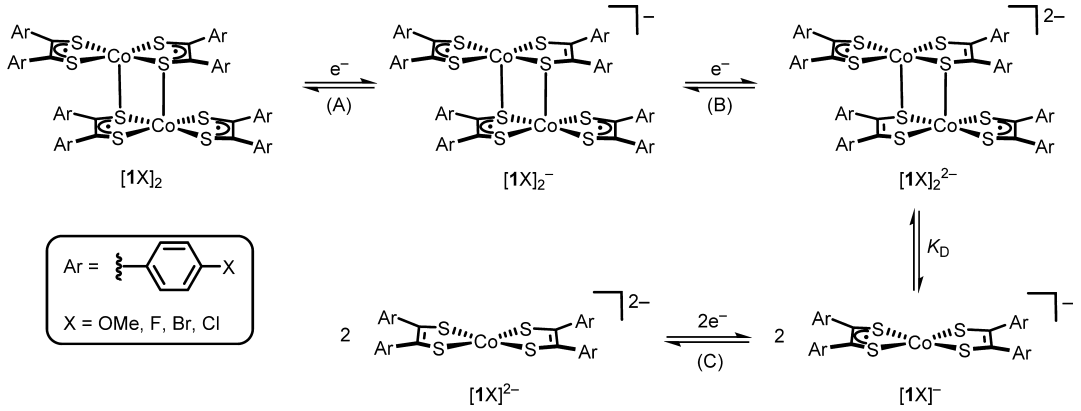

[a]The letters in parentheses correspond to the redox events denoted on the cyclic voltammogram in Figure 3.

Table 1. Redox Potentials (V) Measured for Cobalt-diaryldithiolene Complexes ($[1X]_2$) in DMF Solution with 0.1 M $[NBu_4]PF_6$ as the Supporting Electrolyte

aryl substituent (X)	$E_{1/2}$ ($[1X]_2/[1X]_2^-$)	E_{pc} ($[1X]_2^-/2[1X]^-$)	$E_{1/2}$ ($[1X]^-/[1X]^{2-}$)
Cl	−0.09	−0.67	−1.28
Br	−0.21	−0.69	−1.27
F	−0.30	−0.74	−1.33
OMe	−0.51	−0.98	−1.48

respect to the corresponding value associated with $AnBF_4$ as the proton source. The addition of water to an electrolyte, DMF solution of $[1OMe]_2$ containing 10 mM DCA did not increase the magnitude of the electrocatalytic current, as was reported for $[Ni(P^R_2N^{R'}_2)_2][BF_4]_2$ by DuBois and co-workers.[47]

For soluble proton reduction catalysts such as $[1X]_2$, an interesting question concerns whether the active catalytic species is present in solution or adsorbed onto the electrode surface (or both).[48,49] This issue is generally difficult to conclusively address, although evidence for catalyst adsorption onto the electrode has been observed in some cases, for example, with a number of cobalt-glyoxime derivatives.[50−52] An electrode rinse test was performed to evaluate catalyst homogeneity, in which a glassy carbon electrode was cycled 50 times (from −1.6 to 0.3 V) under electrocatalytic conditions (0.3 mM $NBu_4[1F]$, 12 mM $AnBF_4$). The electrode was then gently rinsed with DMF and subsequently immersed into a fresh electrolyte solution containing 12 mM $AnBF_4$. The rinsed electrode was found to exhibit a reductive current approximately 75% lower in magnitude than in the presence of dissolved $[1X]_2$ (Figure S10 in Supporting Information). These results, suggesting the possible participation of dissolved catalytic species, are consistent with the observed electronic influence of dithiolene aryl substituents on the catalysis (vide supra). However, more detailed investigations are required to accurately characterize the phase of the catalysts in this system. As described below, further experiments in the current study were directed toward isolation of potential catalytic intermediates and evaluation of their competencies in catalysis.

Isolation and Protonation of Intermediates. A more thorough understanding of the chemical properties associated with the reduced cobalt-diaryldithiolene complexes described above would aid in evaluation of these compounds as catalysts and in further catalyst design. Proposed mechanisms for molecular Co HER electrocatalysts generally involve three possible pathways for the H_2-forming step: (1) a dehydrocoupling of two Co(III)−H species to afford H_2 and two Co(II) centers; (2) protonation of a Co(III)−H bond, to directly produce a transient, coordinated H_2 complex; and (3) reduction of Co(III)−H to Co(II)−H, followed by hydride protonation.[53] On the basis of kinetic studies Winkler and co-workers concluded that $[Co(triphos)H(NCMe)_2]^{2+}$ (triphos = 1,1,1-tris(triphenylphosphinomethyl)ethane operates by mechanism 3 involving reduction followed by protonation of a Co(II)−H intermediate.[54] Eisenberg and co-workers have established that Co-diglyoxime catalysts photocatalytically generate H_2 in basic aqueous solution, demonstrating that reduction of a weakly basic Co(III)−H intermediate is likely required for catalysis to proceed.[55] Mechanistic studies by Dempsey and co-workers provide additional kinetic evidence that supports the predominance of a Co(II)−H pathway for Co-diglyoxime catalysts.[56,57] Pathways for catalysis can be altered by experimental conditions, such as acid strength and overpotential. For example, calculations by Fujita[58] and Hammes-Schiffer[59] both provide evidence for Co-diglyoxime derivatives proceeding via a bimetallic pathway (1) in the presence of a weak acid.

To assess the potential role of various reduced species in the catalytic cycle, attempts were made to chemically reduce the $[1X]_2$ complexes, to obtain isolable anionic species for further study. In this context, note that related monoanionic, monomeric M-diaryldithiolene complexes of Fe and Co were previously prepared by addition of a reducing agent (cobaltocene for Fe; borohydride for Co) to the neutral, dimeric precursors.[24,60] For the synthesis of $[1X]^-$ complexes, the neutral dimers were reduced by 1 equiv of KC_8 per Co center, followed by cation metathesis using $[NBu_4]Br$ (Scheme 3). This procedure allowed isolation of $NBu_4[1F]$ in a yield of 83%. Solution magnetic moments for the monoanionic species $NBu_4[1F]$ (μ_{eff} = 2.56 μ_B) and $NBu_4[1Br]$ (μ_{eff} = 2.44 μ_B) are close to the value associated with a single, unpaired electron, suggesting that both the S = 0 and S = 1 states are populated (see Computational Details below). Note that a similar mixture of high- and low-spin states has been suggested for derivatives of $[Co(bdt)_2]^-$.[61] Cyclic voltammetry features for these reduced Co complexes are identical to those of the corresponding neutral dimers, albeit resting potentials were

dx.doi.org/10.1021/ja5019755 | J. Am. Chem. Soc. 2014, 136, 9364−9376

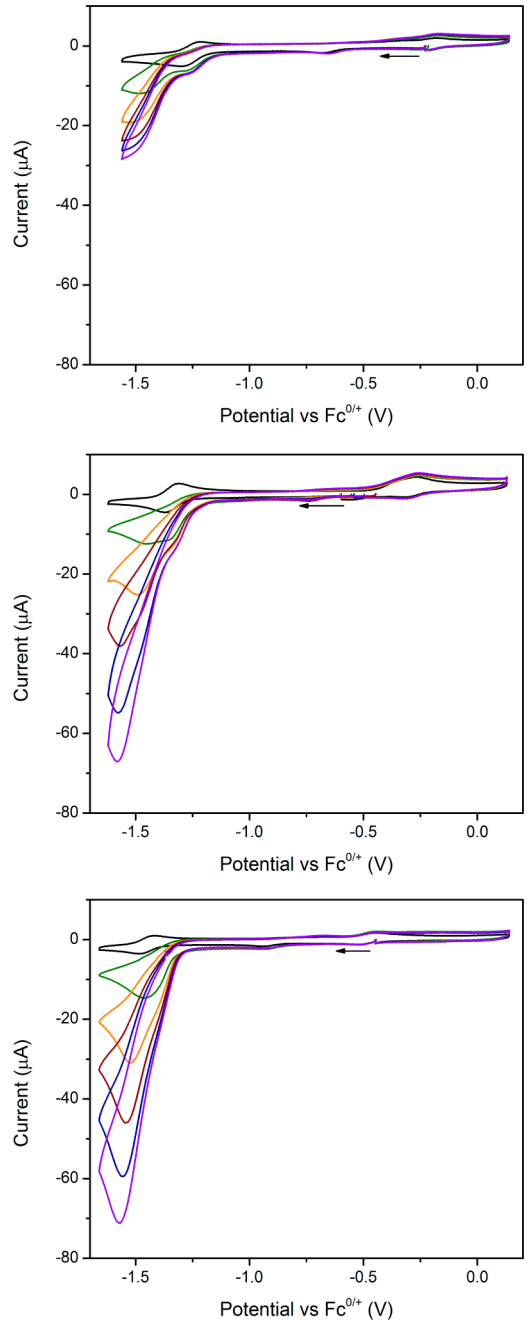

Figure 4. Cyclic voltammograms of $[\mathbf{1}Br]_2$ (top), $NBu_4[\mathbf{1}F]$ (middle), and $[\mathbf{1}OMe]_2$ (bottom) in the presence of increasing equivalents of anilinium tetrafluoroborate. The black trace was acquired in the absence of acid, while each subsequent trace represents the addition of approximately 5 equiv of acid. Conditions: 0.3 mM Co, 0.1 M $[NBu_4]PF_6$ in DMF solution, 0.1 V/s.

observed to shift to the corresponding monoanionic or dianionic reduction events.

Reduction of $[\mathbf{1}F]_2$ with 4 equiv of KC_8 yielded the dipotassium salt $K_2[\mathbf{1}F]$ as a red-orange solid. Evans' method measurement of the magnetic moment for $K_2[\mathbf{1}F]$ in CD_3CN solution afforded a μ_{eff} value of 1.98 μ_B, corresponding most closely to a single unpaired electron. This electronic configuration is consistent with a Co(II) center exhibiting a square planar coordination geometry, which was confirmed by single crystal X-ray crystallography (Figure 5).

Scheme 2. Proposed ECEC Mechanism for the Electrocatalytic Formation of H_2[a]

$$[\mathbf{1}X]^- \overset{e^-}{\rightleftharpoons} [\mathbf{1}X]^{2-}$$

$$[\mathbf{1}X]^{2-} \overset{H^+}{\rightleftharpoons} [\mathbf{1}X(H)]^-$$

$$[\mathbf{1}X(H)]^- \overset{e^-}{\rightleftharpoons} [\mathbf{1}X(H)]^{2-}$$

$$[\mathbf{1}X(H)]^{2-} \overset{H^+}{\rightleftharpoons} [\mathbf{1}X]^- + H_2$$

[a]The H^+ additions can be viewed as protonation at Co to form a Co−H species or dithiolene protonation at sulfur.

The dipotassium salt $K_2[\mathbf{1}F]$ was found to crystallize in the $C2/c$ space group, with cobalt residing on an inversion center. The structure also features potassium ions in η^5-coordination to the CoS_2C_2 chelate ring and additional intermolecular coordination of the potassium ions to the S−Co−S moiety of a neighboring $[\mathbf{1}F]^{2-}$ unit. Observation of this η^5-coordination mode for K^+ is consistent with the presence of a HOMO for the $[\mathbf{1}F]^{2-}$ fragment that is delocalized over the metal and dithiolene ligands (vide infra). This observation suggests that the dithiolene ligand of such dianionic complexes may be protonated at sulfur.[62−65] Acetonitrile molecules were found to bridge neighboring potassium ions, resulting in a two-dimensional coordination polymer in the solid state. The C1−C8 bond in $K_2[\mathbf{1}F]\cdot 2MeCN$ is best described as a double bond, since the bond distance of 1.346(8) Å is just beyond that associated with a typical $C(sp^2)-C(sp^2)$ bond length (1.31−1.34 Å).[66] This short C1−C8 bond distance corresponds to the presence of dithiolate-type ligands. The cyclic voltammogram of $K_2[\mathbf{1}F]$ in DMF solution with a supporting electrolyte of $[NBu_4]PF_6$ exhibits redox features similar to that of the neutral parent complex, $[\mathbf{1}F]_2$ (Figure S1 in Supporting Information). These data suggest that the K^+ ions are not strongly coordinated to $[\mathbf{1}F]^{2-}$ in the electrolyte solution. However, ^1H NMR resonances for $K_2[\mathbf{1}F]\cdot 2MeCN$ in neat acetonitrile-d_3 differ in chemical shift from the NBu_4^+ analogue, $[NBu_4]_2[\mathbf{1}F]$ (vide infra), by ca. 1 ppm, which suggests that K^+ ions may remain in close contact with the dianion in the absence of the $[NBu_4]PF_6$ electrolyte.

To generate a complex that better models the electrochemically observed intermediate, the K^+ ions were exchanged for NBu_4^+. Reduction of $NBu_4[\mathbf{1}F]$ by 1 equiv of KC_8 followed by treatment with $[NBu_4]Br$ afforded $[NBu_4]_2[\mathbf{1}F]$ in a modest yield of 73%. The molecular structure of $[NBu_4]_2[\mathbf{1}F]$ exhibits metrical parameters similar to those of $K_2[\mathbf{1}F]$ (d_{C1-C8} = 1.355(5) Å), and no interaction is observed between the NBu_4^+ counterions and the Co-dithiolene unit (Figure 6, top). A crystallographic inversion center residing on Co enforces an ideal square planar geometry.

Tetrabutylammonium salts of the methoxy- and bromo-substituted mono- and dianionic complexes were generated following a similar route. Although analytically pure samples of $[NBu_4]_2[\mathbf{1}Br]$ could not be isolated, ^1H NMR and electrochemical data are consistent with observations made for the analogous fluoro- and methoxy-derivatized salts. Single crystals suitable for X-ray diffraction were isolated for $[NBu_4]_2[\mathbf{1}Br]$ by layering a THF solution of the salt with hexanes. Interestingly, the molecular structure of $[NBu_4]_2[\mathbf{1}Br]$ was found to deviate from ideal square planar geometry at cobalt, with a dihedral angle (α) between the two ligand (CoS_2) planes of 15° (Figure 6, bottom). This distortion from square planar geometry does

dx.doi.org/10.1021/ja5019755 | J. Am. Chem. Soc. 2014, 136, 9364−9376

Scheme 3. Reductions of Co-diaryldithiolene Species

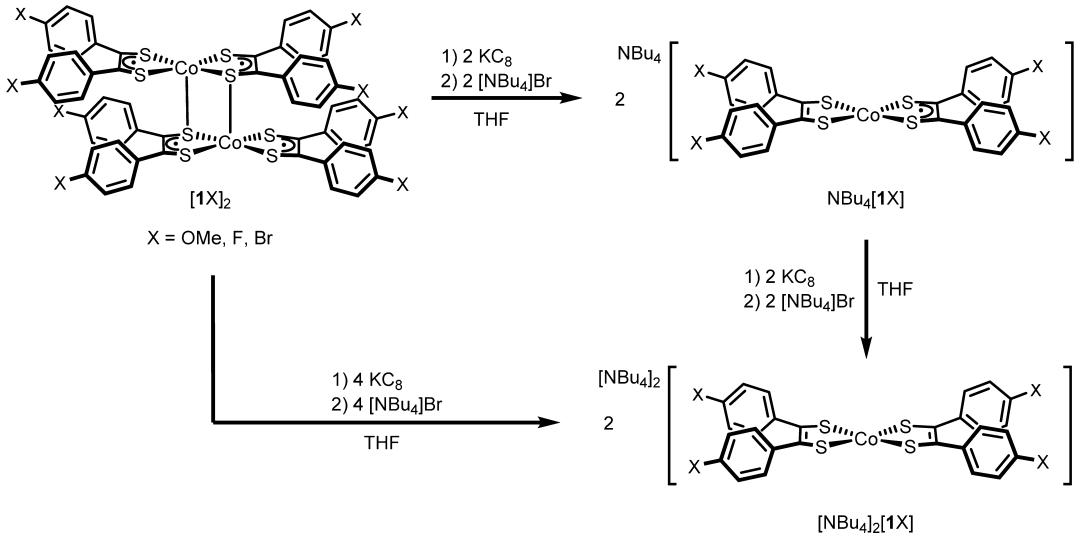

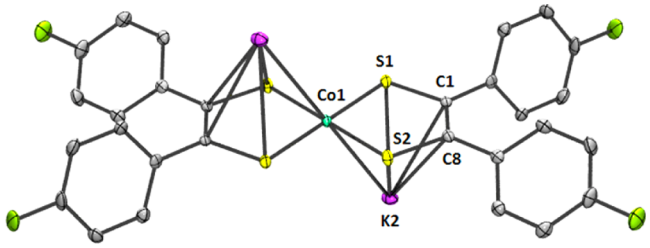

Figure 5. Molecular structure of $K_2[\mathbf{1}F]$ with thermal ellipsoids displayed at a 50% probability level. Hydrogen atoms and acetonitrile solvent molecules have been omitted for clarity.

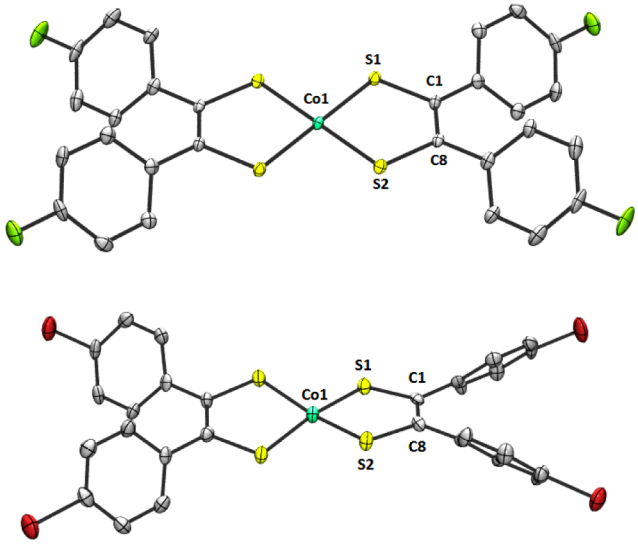

Figure 6. Molecular structures of $[NBu_4]_2[\mathbf{1}F]$ (top) and $[NBu_4]_2[\mathbf{1}Br]$ (bottom), with thermal ellipsoids displayed at a 50% probability level. The NBu_4^+ counterions, hydrogen atoms, and residual solvent molecules have been omitted for clarity.

not appear to be influenced by close contact of the NBu_4^+ counterions. The C1−C8 bond length of 1.358(7) Å for $[NBu_4]_2[\mathbf{1}Br]$ is similar to that of the F-substituted congener.

Protonations of the reduced complexes with $AnBF_4$ were studied by ^1H NMR spectroscopy. Treatment of a DMF-d_7 solution of $[NBu_4]_2[\mathbf{1}F]$ with 1 equiv of $AnBF_4$ at 22 °C was found to afford $NBu_4[\mathbf{1}F]$ and H_2, the latter product being confirmed by gas chromatographic analysis (see Supporting Information). The monoanionic species, $NBu_4[\mathbf{1}F]$, was quantitatively produced, as confirmed using 1,3,5-trimethoxybenzene as an internal standard. The rapid nature of the reaction with acid precluded observation of intermediate Co−H or S−H species. Similar products were observed upon treating $[NBu_4]_2[\mathbf{1}OMe]$ with $AnBF_4$. The addition of $AnBF_4$ to a DMF-d_7 solution of $NBu_4[\mathbf{1}OMe]$ did not result in a shift of the ^1H NMR resonances associated with the Co complex, suggesting that the monoanionic complexes are not protonated.

Two mechanisms leading to the formation of $NBu_4[\mathbf{1}X]$ and H_2 can be imagined, as shown in Scheme 4. Both mechanisms begin with protonation of the dianionic complexes $[NBu_4]_2[\mathbf{1}X]$ to afford the Co−H (rather than an S−H) species, $NBu_4[\mathbf{1}X(H)]$, as supported by computational studies (vide infra). The hydride species might then eliminate H_2 via a bimolecular mechanism to afford $NBu_4[\mathbf{1}X]$ (Scheme 4). An alternative mechanism proceeds via reduction of $NBu_4[\mathbf{1}X(H)]$ to give a dianionic hydride complex $[NBu_4]_2[\mathbf{1}X(H)]$, with $[NBu_4]_2[\mathbf{1}X]$ as the reductant. Protonation of the dianion would then afford $NBu_4[\mathbf{1}X]$ and H_2. Presumably, reduction of $NBu_4[\mathbf{1}X]$ back to the dianionic species $[NBu_4]_2[\mathbf{1}X]$ would close a catalytic cycle for the formation of H_2. The experimental evidence for involvement of $[\mathbf{1}X]^-$ and $[\mathbf{1}X]^{2-}$ species in the mechanism of H^+ reduction is further supported by the computational studies described below.

Computational Studies on the Mechanism of Proton Reduction. Molecular structures for the reduced complexes $NBu_4[\mathbf{1}Br]$ and $[NBu_4]_2[\mathbf{1}Br]$ were used to benchmark the structural models derived from DFT calculations. Further calculations produced a minimized energy model for the monoanionic species $[\mathbf{1}Br]^-$, since the results described above (from electrochemistry and stoichiometric reactivity) indicate that the neutral dimer reductively dissociates prior to catalysis. In agreement with experiment, the DFT calculations (BP86) suggest that singlet and triplet states in $[\mathbf{1}Br]^-$ are close in energy and are rigorously square planar ($\alpha = 0.0°$). The singlet state is found to be slightly lower in energy ($\Delta H = -2.9$ kcal/mol, $\Delta G = -2.0$ kcal/mol). This species has a $\langle S^2 \rangle$ value of 0.3 au, and the cobalt center has a spin density very close to zero,

dx.doi.org/10.1021/ja5019755 | J. Am. Chem. Soc. 2014, 136, 9364−9376

Scheme 4. Plausible Mechanistic Pathways for the Evolution of H_2 via Protonation of the Dianionic Species, $[1X]^{2-}$

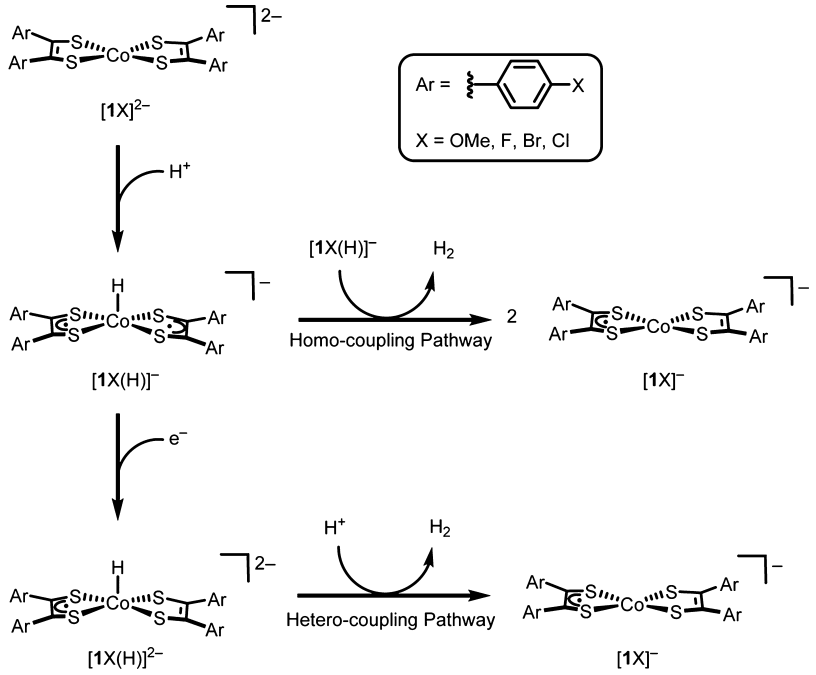

implying an oxidation state of ca. +3. The triplet state that has a spin density on cobalt of 1.30 is best described as a mixture of Co(III) and Co(II) centers, as previously reported for $\{Co[S_2(3,5\text{-}^tBu_2C_6H_2)]_2\}^-$ and $[Co(bdt)_2]^-$.[29] This last point can also explain the main contribution of the ligand-character in the HOMO for the triplet state (53%, Table 2), while the singlet state is mainly metal-centered (66%). Note, however, that the square-planar singlet monoanion is isoenergetic (ΔH = 0.0 kcal/mol; ΔG = −0.1 kcal/mol) with a complex possessing a pseudotetrahedral geometry (Figure S17 in Supporting Information).

Table 2. Percent Cobalt and Sulfur Character of the Highest Occupied Molecular Orbitals (HOMOs) for $[1Br]^-$ and $[1Br]^{2-}$

complex	structure type	multiplicity	M (3d orbital)	S (2p orbital)
$[1Br]^-$	sq planar	singlet	66	16
	pseudo-T_d	singlet	67	15
	sq planar	triplet	17	53
$[1Br]^{2-}$	sq planar	doublet	62	5
	pseudo-T_d	quartet	26	53

Calculations show that the dianionic $[1Br]^{2-}$ species is nearly square planar (α = 22.2°) as an S = 1/2 species, but tetrahedral with a quartet electronic configuration (S = 3/2; α = 88.6°). Interestingly, the low-spin cobalt complex is thermodynamically more stable, by 10.8 kcal/mol (ΔH = +13.6 kcal/mol), which agrees with the single crystal X-ray structure and the solution magnetic moment observed for the analogous salt, $[NBu_4]_2[1F]$ (μ_{eff} = 2.39 μ_B). The HOMO for the square-planar complex is mainly cobalt-centered (62%), and the calculated spin population is 0.81, implying an oxidation state of ca. +2. In addition, we calculated the redox couple associated with reduction of the square-planar monoanion (S = 0) to the square-planar dianion (S = 1/2) for the four different cobalt-diaryldithiolene complexes studied experimentally (Table 3). In this case, the calculated redox potentials are in good agreement with values measured experimentally, which supports the use of the BP86 functional as being appropriate for this study.

Table 3. Calculated Redox Potentials (V) for Cobalt-diaryldithiolene Complexes, [1X] (X = Br, Cl, F, OMe) in Solution (DMF *via* C-PCM Approach)

	$E_{1/2}$			
	$[1Br]^{-/2-}$	$[1Cl]^{-/2-}$	$[1F]^{-/2-}$	$[1OMe]^{-/2-}$
exptl	−1.27	−1.28	−1.33	−1.48
calcd	−1.27[a]	−1.32	−1.38	−1.52

[a] $E_{1/2}[1Br]^{-/2-}$ was used as reference in the isodesmic reactions.

A proposed mechanism for proton reduction by cobalt-diaryldithiolene complexes was further investigated by calculating the products resulting from protonation of $[1Br]^{2-}$ (Scheme 5). The protonation of $[1Br]^{2-}$ at Co was found to be more energetically favorable, to afford the Co−H species $[1Br(H)]^-$ (S = 1/2), than protonation at a ligand sulfur atom (ΔH = +11.6 kcal/mol; ΔG = +10.9 kcal/mol). This result may be explained by the predominance of metal character for the HOMO in $[1Br]^{2-}$ (S = 1/2, 62%). These findings contrast with results reported by Hammes-Schiffer and co-workers for the analogous species $[Co(bdt)_2]^{2-}$, which was found to protonate at sulfur.[25] This discrepancy in predicted reactivity may originate from the difference in starting structures for the dianionic Co complexes, since $[1Br]^{2-}$ possesses a square-planar geometry (experimentally and computationally), whereas $[Co(bdt)_2]^{2-}$ was calculated by Hammes-Schiffer and co-workers as possessing a pseudotetrahedral geometry. Thus, $[1Br]^{2-}$ and $[Co(bdt)_2]^{2-}$ may have different ground-state geometries, but the prediction of a pseudotetrahedral geometry for $[Co(bdt)_2]^{2-}$ may also result from the use of hybrid-functionals (Tables S2 and S3 in Supporting Information). Also, note that a structurally characterized derivative of $[Co(bdt)_2]^{2-}$, $[PPh_4]_2[Co(cbdt)_2]$ (cbdt = 4-cyanobenzene-1,2-dithiolate),[61,67] exhibits a square-planar geometry (α = 1.9°).

dx.doi.org/10.1021/ja5019755 | J. Am. Chem. Soc. 2014, 136, 9364−9376

Scheme 5. Mechanism of H^+ Reduction Catalyzed by Cobalt-diaryldithiolenes Derived from a Combination of Experimental and Theoretical (BP86) Results[a]

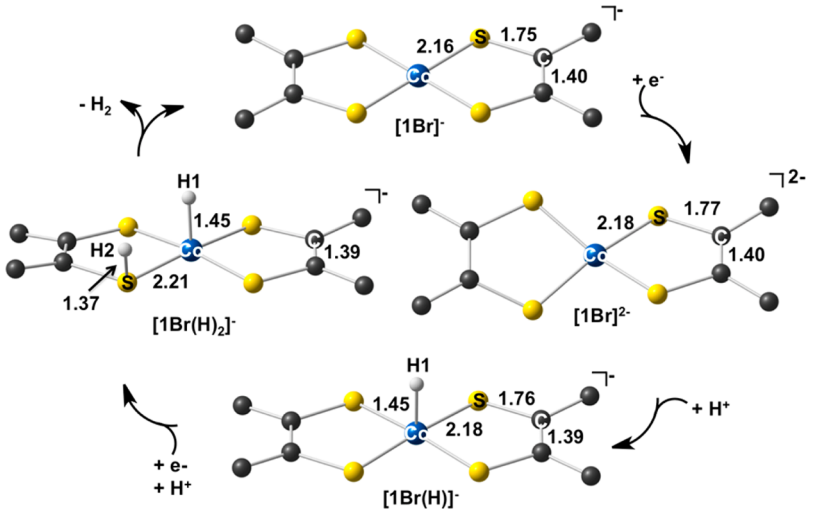

[a]Key distances are in angstroms, and the aryl groups are omitted for clarity.

After protonation of $[1Br]^{2-}$ to give $[1Br(H)]^-$, subsequent reduction and protonation steps are required. In order to determine which of these steps likely occurs first, a reference value is required for the solvation free energy of the proton, $\Delta G_{sol}(H^+)$. To the best of our knowledge an experimental or computed value for $\Delta G_{sol}(H^+)$ is not available in DMF; however, previous studies on derivatives of $[Co(bdt)_2]^-$ additionally support an ECEC mechanism for catalysis,[11,12] implying that reduction of $[1Br(H)]^-$ should be favored over protonation. An alternative mechanism might involve two Co−H complexes that react via a bimolecular process to release H_2. Additionally, a pathway involving a second protonation at a sulfur atom could be possible.

We examined the protonation of the reduced Co−H species, $[1Br(H)]^{2-}$, which was found to give $[1Br(H)_2]^-$, with formation of a S−H bond *syn* to the hydride ligand. This isomer is isoenergetic with the *anti* form with a computed free energy difference of 0.5 kcal/mol in favor of the latter (ΔH = +0.4 kcal/mol); however, the *syn* form positions the two hydrogen atoms in close proximity prior to formation of the H−H bond. The latter process may be viewed as a migration of a proton from sulfur to Co. A transition state structure (S = 0) for transfer of the S−H proton to the metal center was located with a computed free energy of 5.9 kcal/mol ($\Delta\Delta H^{‡}$ = +5.9 kcal/mol, Scheme 6). A Co-dihydrogen species (S = 0) is only −2.3 kcal/mol (ΔH = −1.8 kcal/mol) lower in energy than the previous intermediate, and precedes the release of H_2. A Co-dihydrogen complex with a triplet ground state was also located and found to be lower in energy ($\Delta\Delta H$ = −6.2 kcal/mol; $\Delta\Delta G$ = −6.7 kcal/mol) than the singlet state; however, the transition state corresponding to transfer of the S−H proton was found to be +9.9 kcal/mol ($\Delta\Delta H^{‡}$ = +11.1 kcal/mol) higher in energy in the triplet electronic configuration.

Scheme 6. Computed Free Energy Profile (kcal/mol, DMF Solution) for the Singlet Ground State Displaying Migration of a Proton in $[1Br(H)_2]^-$ from a Sulfur Atom to the Co−H Bond[a]

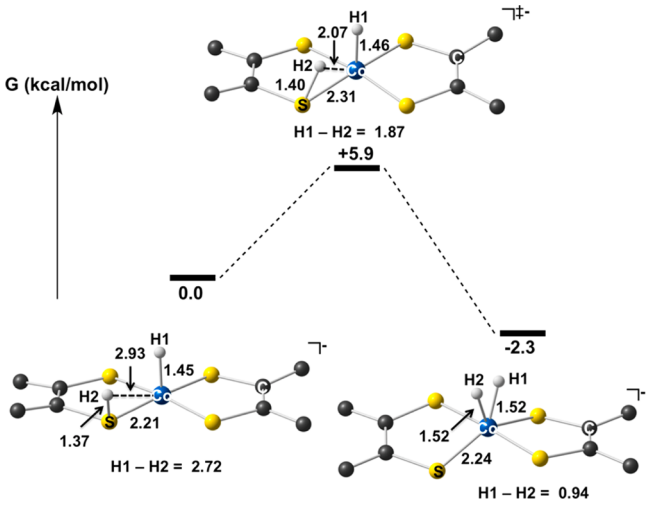

[a]Key distances are displayed in angstroms. Aryl groups have been omitted for clarity.

CONCLUDING REMARKS

Electrochemical analyses of various cobalt-diaryldithiolene derivatives reveal that the *para*-aryl substitutent modulates the potential at which catalysis is observed and significantly influences the magnitude of the electrocatalytic current. A likely mechanism for catalytic proton reduction by cobalt-diaryldithiolene species has been delineated, via corroboration of stoichiometric chemical transformations with DFT-predicted pathways (Scheme 5). This catalysis appears to involve the "doubly reduced" dianionic species $[1X]^{2-}$, for which the negative charge is effectively delocalized by the redox-active ligand set. Experimentally, it was determined that these dianionic cobalt-diaryldithiolene complexes exhibit a square planar geometry in solid form and in solution. Furthermore, the coordination geometry of the cobalt complex was found to dramatically affect the site of protonation for the dianionic species. For the square planar geometry, protonation at Co is preferred, whereas the pseudotetrahedral complex undergoes protonation at sulfur. The dianionic $[NBu_4]_2[1X]$ salts were found to evolve H_2 upon treatment with acid, and cyclic voltammetry suggests that this process involves reduction of an

dx.doi.org/10.1021/ja5019755 | J. Am. Chem. Soc. 2014, 136, 9364−9376

initially protonated dianion, $[\mathbf{1}X(H)]^-$, to $[\mathbf{1}X(H)]^{2-}$ prior to hydrogen evolution. By DFT calculations, the latter step appears to be involved in electrocatalysis, and in the reaction of $[\mathbf{1}X]^{2-}$ with acid, this reduction would require an electron transfer from unreacted dianion. The lack of an EC′ mechanism, whereby a Co−H species is directly protonated to form a dihydrogen adduct, is presumably a consequence of the delocalized nature of the HOMO for $[\mathbf{1}X(H)]^-$ (cf. 21% metal d-orbital in $[\mathbf{1}Br(H)]^-$), which renders the hydride weakly basic. Protonated intermediates, Co−H or S−H, were not observed by ^{1}H NMR spectroscopy in the stoichiometric acid experiments. Cobalt hydrides of active proton reduction catalysts tend to be unstable due to their propensity to generate hydrogen via homo-coupling,[4,68] but isolated, phosphine-ligated Co−H complexes have been reported.[54,69]

The results reported here highlight the strong electronic interplay between the metal center and dithiolene ligands in cobalt-diaryldithiolene complexes. Although the redox non-innocence of the diaryldithiolene ligands enables the isolation of dianionic cobalt-tetrathiolates at fairly mild reduction potentials (over the range of −1.3 to −1.5 V), the poor donor strength of the dithiolenes necessitates an additional reduction step to observe catalytic proton reduction. Thus, the more donating complex $[\mathbf{1}OMe]^{2-}$ was found to exhibit a larger magnitude of catalytic current, as compared to the more electron-poor, halide-substituted dithiolene derivatives. The development of cobalt-dithiolene catalysts exhibiting greater disparity between Co and dithiolene orbital energy levels may result in improved proton reduction activity.

EXPERIMENTAL SECTION

General Considerations. *Caution: IBX has been demonstrated to be explosive upon impact or by heating to temperatures above 200 °C.*[70] All experiments were performed under an atmosphere of N_2 in a drybox or using standard Schlenk techniques. Potassium graphite,[71] IBX,[72] and $[\mathbf{1}OMe]_2$[24] were prepared according to literature methods. Tetrahydrofuran, *o*-difluorobenzene, acetonitrile, and hexane were purified using a Jorge C. Meyer solvent purification system and stored over 3 Å sieves. 4,4′-Dibromobenzil (Alfa Aesar), 4,4′-difluorobenzil (Acros), 4-chlorobenzaldehyde (Alfa Aesar), and aniline (Sigma-Aldrich) were used without further purification. Acetonitrile-d_3 was dried over CaH_2 and distilled. All NMR experiments were conducted on a Bruker Avance 500 instrument at the following frequencies: ^{1}H = 500 MHz, ^{13}C = 125.7 MHz, and ^{19}F = 470 MHz. All chemical shifts are referenced against the residual proteo-solvent resonance. Infrared spectroscopy measurements were acquired on either a Nicolet Avatar 360 FT-IR with an attenuated total reflectance (ATR) accessory or a Bruker Vertex 70 FT-IR. Magnetic susceptibility measurements were made using Evans' method.[73] An NMR tube containing the paramagnetic compound in deuterated solvent was fitted with an insert containing a neat sample of the same deuterated solvent. The paramagnetic shift of the residual solvent signal was used to calculate the room temperature solution magnetic moment. High-resolution mass spectrometry data was acquired using an Agilent Technologies 6230 LC−MS.

Electrochemistry. All electrochemical experiments were performed using a Bio-Logic Systems SP-200 potentiostat. Cyclic voltammetry experiments were performed using $[NBu_4]PF_6$ (Sigma-Aldrich, recrystallized from acetone/ethanol) as an electrolyte, a 3 mm glassy carbon working electrode, a graphite rod counter electrode, and a nonaqueous reference electrode containing a Ag wire immersed into an MeCN solution of 0.1 M $[NBu_4]PF_6$ and 0.01 M $Ag/AgNO_3$. The reference electrode was separated from the cell's contents by a Vycor frit. Bulk electrolysis experiments were performed in a custom two-compartment cell that separates the counter electrode from the analyte via a glass frit of fine porosity. The working electrode was a glassy carbon rod (5 mm diameter) purchased from Alfa Aesar, and the reference electrode was a nonaqueous reference containing a Ag wire immersed into an MeCN solution of 0.1 M $[NBu_4]PF_6$ and 0.01 M $Ag/AgNO_3$. Bulk electrolysis experiments were conducted using 0.3 mM Co catalyst and 15 mM acid. Experiments were conducted over a period of 2 h, during which approximately 30 C of charge had passed. Faradaic yields were measured by flowing Ar through the headspace of the electrolysis cell (at a measured, constant rate) that was directly connected to an Agilent 490 micro gas chromatograph employing a carrier gas of N_2.

X-ray Crystallography. Data collection was performed on single crystals coated with Paratone-N oil and mounted on Kaptan loops. The crystals were frozen under a stream of N_2 (100 K; Oxford Cryostream 700) during measurements. Data were collected using a Bruker APEX II QUAZAR diffractometer equipped with a Microfocus Sealed Source (Incoatec IμS; Mo Kα λ = 0.71073 Å) and APEX-II detector. Raw data were integrated and corrected for Lorentz and polarization effects using Bruker APEX2 v. 2009.1.[74] Absorption corrections were applied using SADABS.[75] Space group assignments were determined by examination of systematic absences, E-statistics, and successive refinement of the structures. Structures were solved using direct methods and refined by least-squares refinement on F^2 followed by difference Fourier synthesis.[76] All hydrogen atoms were included in the final structure factor calculation at idealized positions and were allowed to ride on the neighboring atoms with relative isotropic displacement coefficients. Thermal parameters were refined anisotropically for all non-hydrogen atoms. Experimental details of the crystal structures for $[\mathbf{1}Br]_2$, $NBu_4[\mathbf{1}Br]_2$, $NBu_4[\mathbf{1}Br]$, $[NBu_4]_2[\mathbf{1}Br]$, $K_2[\mathbf{1}F]\cdot 2MeCN$, $[NBu_4]_2[\mathbf{1}F]$, and $NBu_4[\mathbf{1}OMe]$ are given in Table S1 in Supporting Information. Additional details can be found in the CIF files available as electronic Supporting Information. Although $[NBu_4]_2[\mathbf{1}OMe]$ crystallizes readily, the obtained crystals were repeatedly of low quality; however, the connectivity of the complex could be established unambiguously. The following structures deserve further explanation. During the final stage of refinement for $[NBu_4]_2[\mathbf{1}F]$ small residual electron density peaks (~2e$^-$) were present. This was interpreted as disordered and not fully occupied hexanes molecules (mixture of isomers), and the SQUEEZE routine as implemented in the PLATON suite was utilized to remove 51e$^-$ from a total void volume of 196 Å^3. This corresponds roughly to 0.6 molecules of hexanes per unit cell. In the structure of $NBu_4[\mathbf{1}OMe]$, one of the substituted phenyl rings (C19−C24) showed out of plane distortion that resulted in significantly elongated ellipsoids for two of the carbon atoms upon anisotropic refinement of their thermal parameters. The ShelX constraint EADP for all carbons of this aromatic ring was utilized to increase the ellipsoid parameters. Additionally, residual electron density (36e$^-$ in 136 A^3) corresponding to roughly one THF solvent molecule per unit cell was removed using the SQUEEZE routine. The tetrabutyl ammonium counterion in the structure of $NBu_4[\mathbf{1}Br]_2$ crystallized with the N atom on a special position (inversion center), and both crystallographically independent butyl groups are disordered over two positions with a ~50/50 ratio. The disorder could be modeled and stable and freely anisotropically refined without the use of any restraints/constraints. In the structure of $NBu_4[\mathbf{1}Br]$ one-half of 1.5 THF molecules in the asymmetric unit is disordered over at least two positions. Anisotropic refinement of the C and O atoms (using the EADP restraint) was stable, and the highest electron density peaks (Q1 = 1.03e$^-$/A^3) were, as expected, subsequently observed around the heavy Br atoms of the ligand.

$[Co(S_2C_2(p\text{-}FC_6H_4)_2)_2]_2$ ($[\mathbf{1}F]_2$). 1,4-Dioxane (15 mL) was added to a flask containing 4,4′-difluorobenzil (0.50 g, 2.0 mmol) and phosphorus pentasulfide (1.4 g, 3.0 mmol). The yellow mixture was heated at reflux for 18 h. The resulting tan slurry was filtered while hot via cannula into a degassed, aqueous solution of $CoCl_2\cdot 6H_2O$ (2.0 mL, 0.50 M), yielding a dark green mixture that was heated to 90 °C for 2 h. After cooling to room temperature, the suspended, dark green solid was isolated by filtration. The isolated dark green solids were washed with water (50 mL) and pentane (50 mL) and dried under vacuum. Yield = 0.24 g (39%). ^{1}H NMR (tetrahydrofuran-d_8): δ 7.28−7.21 (m, 8H), 7.04−6.97 (m, 8H). ^{19}F NMR (tetrahydrofuran-d_8): δ −113.0

dx.doi.org/10.1021/ja5019755 | J. Am. Chem. Soc. 2014, 136, 9364−9376

(s). Anal. Calcd for $C_{56}H_{32}CoF_8S_8$: C, 54.63; H, 2.62. Found C, 54.25; H, 2.51.

1,2-Bis(4-chlorophenyl)ethane-1,2-diol (Diastereomeric Mixture). Titanium(IV) tetrachloride (3.14 mL, 28.6 mmol) was added dropwise to a slurry of Mn powder (3.14 g, 57.2 mmol) in THF (60 mL) at −5 °C. The resulting dark green slurry was warmed to room temperature, followed by heating to reflux for a period of 2 h. The dark brown mixture was cooled to −5 °C and treated with a THF solution of *p*-chlorobenzaldehyde (20 mL, 0.57 M). The dark brown mixture was stirred at −5 °C and was monitored by TLC. After 45 min, the reaction mixture was warmed to room temperature and poured into a saturated, aqueous solution of $NaHCO_3$ (30 mL). After the quenched reaction mixture stirred for 1 h, it was filtered, and the resulting solids were washed with diethyl ether (50 mL). The biphasic filtrate was separated in a funnel, and the aqueous layer was extracted with additional portions of Et_2O (2 × 50 mL). The combined Et_2O extracts were dried over $MgSO_4$, filtered, and concentrated to afford off-white solids. Purification of the crude material was accomplished by silica gel chromatography, using an eluent of 3:1 hexanes/EtOAc. Yield = 0.84 g (52%). ^{1}H NMR (dichloromethane-d_2): δ 7.25 (d, J = 8.3 Hz, 4 H, diast b), 7.22 (d, J = 8.0 Hz, 4 H, diast a), 7.11 (d, J = 8.3 Hz, 4 H, diast b), 7.04 (d, J = 8.0 Hz, 4 H, diast a), 4.83 (s, 2 H, diast b, C*H*OH), 4.61 (s, 2 H, diast a, C*H*OH), 3.03 (s, 2 H, diast a, CHO*H*), 2.52 (s, 2 H, diast b, CHO*H*). ^{13}C NMR (dichloromethane-d_2): δ 138.8 (diast a), 138.7 (diast b), 133.9 (diast a), 133.8 (diast b), 128.9 (diast b), 128.8 (diast a), 128.6 (diast a), 128.5 (diast b), 78.8 (diast a), 77.4 (diast b). Anal. Calcd for $C_{14}H_{12}Cl_2O_2$: C, 59.39; H, 4.27. Found: C, 59.30; H, 4.14.

4,4′-Dichlorobenzil. A slurry of 2-iodoxybenzoic acid (IBX) (2.99 g, 10.7 mmol) in DMSO (5 mL) was stirred over a period of 20 min to afford a colorless solution. A THF solution of 1,2-bis(4-chlorophenyl)-ethane-1,2-diol (10 mL, 0.43 M, mixture of diastereomers) was added to the DMSO solution of IBX to yield a bright yellow solution. The bright yellow solution was stirred over a period of 1 h, during which a colorless precipitate formed. A saturated, aqueous solution of $NaHCO_3$ (50 mL) was added to the yellow slurry to quench the reaction. The resulting yellow mixture was extracted with CH_2Cl_2 (2 × 50 mL). The combined CH_2Cl_2 extracts were washed with multiple portions of water (2 × 50 mL) and brine (3 × 50 mL), followed by drying over $MgSO_4$. The $MgSO_4$ was removed via filtration, and the yellow filtrate was concentrated under vacuum to afford a yellow solid. Recrystallization of the product was achieved by dissolving the yellow solid in boiling Et_2O and cooling the resulting solution to −20 °C. The resulting yellow crystals were isolated via filtration and dried under vacuum. Yield = 0.66 g (55%). ^{1}H NMR (chloroform-*d*): δ 7.92 (d, J = 8.2 Hz, 4 H), 7.50 (d, J = 8.2 Hz, 4 H). ^{13}C NMR (chloroform-*d*): δ 192.4, 141.8, 131.2, 131.1, 129.5. IR (KBr): ν_{CO} = 1691 cm^{-1} (s). Anal. Calcd for $C_{14}H_8Cl_2O_2$: C, 60.24; H, 2.89. Found: C, 60.49; H, 2.69.

[Co(S$_2$C$_2$(*p*-ClC$_6$H$_4$)$_2$)$_2$]$_2$ ([1Cl]$_2$). This complex was prepared using the method described for [1F]$_2$, from 4,4′-dichlorobenzil (0.60 g, 2.1 mmol), phosphorus pentasulfide (1.4 g, 3.2 mmol), and $CoCl_2{\cdot}6H_2O$ (0.25g, 1.0 mmol). Further purification of the product involved boiling the dark green solids in MeOH (5 mL), followed by filtration of the hot mixture. The isolated dark green solid was washed with Et_2O and dried under vacuum. Yield = 0.22 g (30%). ^{1}H NMR (dichloromethane-d_2): δ 7.25 (d, J = 8.4 Hz, 16 H), 7.19 (d, J = 8.5 Hz, 16 H). Anal. Calcd for $C_{56}H_{32}CoCl_8S_8$: C, 49.35; H, 2.37. Found: C, 49.72; H, 2.70.

[Co(S$_2$C$_2$(*p*-BrC$_6$H$_4$)$_2$)$_2$]$_2$ ([1Br]$_2$). This complex was prepared using the method described for [1F]$_2$, from 4,4′-dibromobenzil (1.5 g, 4.1 mmol), phosphorus pentasulfide (2.7 g, 6.1 mmol), and $CoCl_2{\cdot}6H_2O$ (0.47 g, 2.0 mmol). Further purification of the product involved boiling the solids in MeOH (10 mL), followed by filtration of the hot mixture. The isolated dark green solid was washed with Et_2O and dried under vacuum. Yield = 0.56 g (32%). ^{1}H NMR (dichloromethane-d_2): δ 7.41 (d, J = 7.9 Hz, 16 H), 7.12 (d, J = 8.0 Hz, 16 H). Anal. Calcd for $C_{56}H_{32}Br_8CoS_8$: C, 39.14; H, 1.88. Found: C, 38.85; H, 1.54.

NBu$_4$[Co(S$_2$C$_2$(*p*-OMeC$_6$H$_4$)$_2$)$_2$] (NBu$_4$[1OMe]). A solution/suspension of [1OMe]$_2$ (150 mg, 0.11 mmol) in THF (10 mL) was cooled to −30 °C, and then KC_8 (32 mg, 0.24 mmol) was added. The resulting red mixture was warmed to room temperature and stirred over a period of 1 h. The dark red mixture was treated with [NBu$_4$]Br (73 mg, 0.23 mmol) and subsequently stirred for 22 h at room temperature. The dark red-brown mixture was filtered through a ∼2 cm pad of Celite. The Celite was washed with THF (10 mL), and the resulting dark red-brown filtrate was concentrated under reduced pressure to yield a red-brown residue. Dissolution of the residue into a minimal amount of THF, followed by layering with hexane afforded the desired product as dark red crystals suitable for X-ray diffraction. Yield = 150 mg (75%). ^{1}H NMR (*N*,*N*-dimethylformamide-d_7): δ 16.06 (d, J = 7.0 Hz, 8 H), 13.02 (d, J = 6.1 Hz, 8 H), 6.25 (s, 12 H), 2.80 (t, J = 8.2 Hz, 8 H), 1.30 (p, J = 7.8 Hz, 8 H), 1.17 (h, J = 7.2 Hz, 8 H), 0.82 (t, J = 7.2 Hz, 12 H). Anal. Calcd for $C_{48}H_{64}CoNO_4S_4$: C, 63.62; H, 7.12; N, 1.55. Found: C, 63.52; H, 7.44; N, 1.67.

NBu$_4$[Co(S$_2$C$_2$(*p*-FC$_6$H$_4$)$_2$)$_2$] (NBu$_4$[1F]). This complex was prepared using the method described for NBu$_4$[1OMe], from [1F]$_2$ (175 mg, 0.14 mmol), KC_8 (60 mg, 0.30 mmol), and [NBu$_4$]Br (92 mg, 0.28 mmol) to afford the desired product as a dark brown solid. The dark red-brown solid was dissolved in a minimum amount of THF and layered with hexane to afford a dark red-brown, crystalline solid. Yield = 200 mg (83%). ^{1}H NMR (acetonitrile-d_3): δ 15.60 (br s, 8 H), 12.38 (br s, 8 H), 2.40 (br t, 8H), 1.14−1.02 (br m, 16 H), 0.79 (br t, 12 H). ^{19}F{^{1}H} NMR (acetonitrile-d_3): δ −107 (s). ^{1}H NMR (*N*,*N*-dimethylformamide-d_7): δ 16.63 (br s, 8 H), 13.36−13.27 (m, 8 H), 3.04−2.97 (m, 8 H), 1.51−1.39 (br m, 8 H), 1.31−1.19 (m, 8 H), 0.87 (t, J = 7.2 Hz, 12 H). ^{19}F{^{1}H} NMR (*N*,*N*-dimethylformamide-d_7): δ −105 (s). Effective magnetic moment (*N*,*N*-dimethylformamide-d_7, 295 K): μ_{eff} = 2.56 μ_B. Anal. Calcd for $C_{44}H_{52}CoNF_4S_4$: C, 61.59; H, 6.11; N, 1.63. Found: C, 61.33; H, 5.74; N, 1.99.

NBu$_4$[Co(S$_2$C$_2$(*p*-BrC$_6$H$_4$)$_2$)$_2$] (NBu$_4$[1Br]). This complex was prepared using the method described for NBu$_4$[1OMe], from [1Br]$_2$ (100 mg, 0.06 mmol), KC_8 (17 mg, 0.12 mmol), and [NBu$_4$]Br (38 mg, 0.12 mmol) to afford the desired product as a dark brown solid. Dark brown crystals suitable for X-ray diffraction were grown via diffusion of hexanes into a THF solution of NBu$_4$[1Br]. Yield = 95 mg (72%). ^{1}H NMR (*N*,*N*-dimethylformamide-d_7): δ 15.97 (s, 8 H), 13.43 (s, 8 H), 3.06−2.96 (m, 8 H), 1.50−1.40 (m, 8 H), 1.24 (h, J = 7.4 Hz, 8 H), 0.86 (t, J = 7.3 Hz, 12 H). Effective magnetic moment (*N*,*N*-dimethylformamide-d_7, 295 K): μ_{eff} = 2.44. μ_B Anal. Calcd for $C_{44}H_{52}Br_4CoNS_4$: C, 47.97; H, 4.76; N, 1.27. Found: C, 47.85; H, 4.53; N, 1.24.

K$_2$[Co(S$_2$C$_2$(*p*-FC$_6$H$_4$)$_2$)$_2$]·2MeCN (K$_2$[1F]·2MeCN). A THF solution of [1F]$_2$ (150 mg, 0.12 mmol) was cooled to −30 °C and treated with KC_8 (34 mg, 0.25 mmol). After stirring for 20 min, a second portion of KC_8 (34 mg, 0.25 mmol) was added to afford a golden orange suspension. The suspension was stirred over a period of 1 h while equilibrating to room temperature, and then filtered through a ∼3 cm pad of Celite. The Celite was washed with additional THF (30 mL) and the combined, dark-orange filtrates were concentrated to dryness to afford a metallic-orange solid. The orange solid was dissolved in a 1:1 mixture of MeCN:Et_2O, layered with hexane, and cooled to −30 °C to afford red-orange, X-ray quality crystals. Yield = 81 mg (59%). ^{1}H NMR (acetonitrile-d_3): δ 6.49 (br s, 8 H), 6.12 (br s, 8 H). Anal. Calcd for $C_{32}H_{22}CoF_4K_2N_2S_4$: C, 49.53; H, 2.86; N, 3.61. Found: C, 49.42; H, 2.63; N, 3.34.

[NBu$_4$]$_2$[Co(S$_2$C$_2$(*p*-OMeC$_6$H$_4$)$_2$)$_2$] ([NBu$_4$]$_2$[1OMe]). Route A. A solution/suspension of [1OMe]$_2$ (150 mg, 0.11 mmol) in THF (10 mL) was cooled to −30 °C, and then KC_8 (64 mg, 0.47 mmol) was added. The green mixture was warmed to room temperature and stirred over a period of 1 h. The resulting dark-orange mixture was treated with [NBu$_4$]Br (146 mg, 0.23 mmol) and subsequently stirred for 22 h. The dark orange mixture was evaporated to dryness to afford an orange residue. The orange residue was extracted into 10 mL of *o*-difluorobenzene and filtered through a ∼3 cm pad of Celite. The Celite was washed with 10 mL of *o*-difluorobenzene, and the dark orange filtrate was concentrated under vacuum to a volume of ca. 10 mL. Layering of the filtrate with hexanes, followed by cooling to −30 °C afforded the desired product as dark brown crystals. Yield = 175 mg (69%). **Route B.** A solution of NBu$_4$[1OMe] (80 mg, 0.088 mmol) in THF (7 mL) was cooled to −30 °C, and then KC_8 (12 mg, 0.093

dx.doi.org/10.1021/ja5019755 | J. Am. Chem. Soc. 2014, 136, 9364−9376

mmol) was added. The resulting dark orange mixture was stirred while equilibrating to room temperature. After 1 h of stirring, the dark orange mixture was treated with [NBu_4]Br (28 mg, 0.088 mmol) and subsequently stirred for 20 h. The dark orange suspension was filtered through a ∼3 cm pad of Celite. The Celite was washed with 10 mL of THF, and the dark orange filtrate was concentrated under vacuum to a volume of ca. 10 mL. Layering of the filtrate with hexanes afforded the desired product as a dark brown, crystalline solid. Yield = 70 mg (69%). ^{1}H NMR (*N*,*N*-dimethylformamide-d_7): δ 7.53 (br s, 8 H), 6.65 (br s, 8 H), 3.89 (br s, 12 H), 1.45 (br s, 16 H), 1.29 (br s, 16 H), 1.15 (br s, 16 H), 1.06 (br s, 24 H). Anal. Calcd for $C_{64}H_{100}CoN_2O_4S_4$: C, 66.92; H, 8.77; N, 2.44. Found: C, 66.53; H, 8.96; N, 2.14.

[NBu_4]$_2$[Co(S_2C_2(*p*-FC_6H_4)$_2$)$_2$] ([NBu_4]$_2$[1F]). This complex was prepared using Route B described for [NBu_4]$_2$[1OMe], from NBu_4[1F] (100 mg, 0.12 mmol), KC_8 (17 mg, 0.13 mmol), and [NBu_4]Br (38 mg, 0.12 mmol) to afford the desired product as a dark, red-brown solid. Layering a (1:1) MeCN/*o*-difluorobenzene solution of the product with hexanes afforded the product as dark brown crystals. Yield = 55 mg (42%). Dark brown crystals suitable for X-ray diffraction were grown via vapor diffusion of hexanes into an *o*-difluorobenzene solution of [NBu_4]$_2$[1F]. ^{1}H NMR (*N*,*N*-dimethylformamide-d_7): δ 5.75 (br s, 8 H), 5.38 (br s, 8 H), 2.97 (br s, 16 H), 1.38 (br s, 16 H), 1.16 (br s, 16 H), 0.90 (br s, 24 H). ^{19}F{^{1}H} NMR (*N*,*N*-dimethylformamide-d_7): δ −125 (br s). Effective magnetic moment (*N*,*N*-dimethylformamide-d_7, 295 K): μ_{eff} = 2.39 μ_B. Anal. Calcd for $C_{60}H_{88}CoF_4N_2S_4$: C, 65.48; H, 8.06; N, 2.55. Found: C, 65.50; H, 7.74; N, 2.54.

[NBu_4]$_2$[Co(S_2C_2(*p*-BrC_6H_4)$_2$)$_2$] ([NBu_4]$_2$[1Br]). This complex was prepared using Route A, as described for [NBu_4]$_2$[1OMe], from [1Br]$_2$ (150 mg, 0.087 mmol), KC_8 (48 mg, 0.36 mmol), and [NBu_4]Br (112 mg, 0.35 mmol) to afford the desired product as a dark brown solid. Yield = 130 mg (55%). Dark brown crystals suitable for X-ray diffraction were grown via vapor diffusion of hexanes into a THF solution of [NBu_4]$_2$[1Br]. ^{1}H NMR (*N*,*N*-dimethylformamide-d_7): δ 5.93 (br s, 8 H), 5.63 (br s, 8 H), 3.13 (br s, 16 H), 1.51 (br s, 16 H), 1.23 (br s, 16 H), 0.92 (br s, 24 H). HRMS (ESI-TOF) *m*/*z*: [M + NBu_4]$^-$ calcd for $C_{44}H_{52}Br_4CoNS_4$ 1096.9048, found 1096.8990. Analytically pure samples of [NBu_4]$_2$[1Br] could not be isolated. ^{1}H NMR aryl C−*H* resonances for [NBu_4]$_2$[1Br] exhibit chemical shifts similar to those observed for [NBu_4]$_2$[1F]. The cyclic voltammogram of [NBu_4]$_2$[1Br] is identical to that of [1Br]$_2$, and no electroactive impurities were observed. The cyclic voltammogram of [1Br]$_2$ in THF solution displays an additional irreversible reduction event exhibiting an onset potential of −2.77 V, hinting that over-reduction is possible. Attempts to generate [NBu_4]$_2$[1Br] using [Fp]$^-$ ([Fp]$^-$ = [(C_5H_5)-Fe(CO)$_2$]$^-$, $E_{1/2}$ = −1.8 V in THF)[77] as an alternative reducing agent afforded similar samples.

Computational Details. DFT was employed in conjunction with the experimental results to elucidate a probable mechanism of catalytic proton reduction by the Co-diaryldithiolene species studied (Scheme 5). DFT calculations were performed with the Q-Chem package[78] using the BP86 functional.[79,80] Additional test calculations on the extent to which the results are functional-dependent were also performed using the B3LYP[81,82] and wB97X[83] functionals (Tables S2 and S3 in Supporting Information). The Wachters+f basis set[84,85] was used for Co, and the double-ζ polarized plus diffuse 6-31+G** basis was used for all other atoms.[86,87] Additional calculations with the triple-ζ polarized plus diffuse 6-311++G** basis showed similar results (Tables S6−S8 in Supporting Information). Atomic coordinates acquired from X-ray structures of the monoanionic and dianionic monomers reported herein were used as the initial input for calculations. Exchange correlation integrals were evaluated with a quadrature grid of 75 radial points and 302 Lebedev angular points. Unrestricted SCF calculations were performed using a matrix element threshold of 10^{-14} hartrees and a tight convergence criterion of 10^{-8} hartrees via either the Direct Inversion in the Iterative Subspace (DIIS) algorithm[88,89] or the Geometric Direct Minimization (GDM) algorithm.[90] Stability analyses were performed in addition to analytical frequency calculations on all stationary points to ensure that geometries correspond to local minima (all positive eigenvalues) or transition state (one negative eigenvalue). IRC calculations and subsequent geometry optimizations were used to confirm the minima linked by each transition state. Single-point calculations including solvent-corrected energies have also been computed via the SWIG C-PCM approach[91,92] (DMF, ε = 37.219) using the UFF radii. All energies are corrected for zero-point vibrational energy, while free energies (quoted at 298.15 K and 1 atm) are corrected using the modified harmonic oscillator approximation proposed by Grimme where low-lying vibrational modes are treated by a free-rotor approximation.[93]

■ ASSOCIATED CONTENT

Ⓢ Supporting Information

Additional electrochemical data, infrared spectroscopy and mass spectrometry data, tabulated X-ray data, and experimental details for protonation studies. Molecular structures for NBu_4[1Br]$_2$, NBu_4[1Br], and NBu_4[1OMe] acquired from single crystal X-ray diffraction data. Additional computational data. This material is available free of charge via the Internet at http://pubs.acs.org.

■ AUTHOR INFORMATION

Corresponding Authors

mhg@cchem.berkeley.edu
tdtilley@berkeley.edu

Notes

The authors declare no competing financial interest.

■ ACKNOWLEDGMENTS

This material is based upon work performed by the Joint Center for Artificial Photosynthesis, a DOE Energy Innovation Hub, supported through the Office of Science of the U.S. Department of Energy under Award Number DE-SC0004993. The authors would like to thank Dr. Michael Nippe for assistance with X-ray crystallography and Dr. Andreas Hauser for helpful discussions.

■ REFERENCES

(1) Gray, H. B. *Nat. Chem.* **2009**, *1*, 7.
(2) Lewis, N. S.; Nocera, D. G. *Proc. Natl. Acad. Sci. U.S.A.* **2006**, *103*, 15729.
(3) Hu, X.; Cossairt, B. M.; Brunschwig, B. S.; Lewis, N. S.; Peters, J. C. *Chem. Commun.* **2005**, 4723.
(4) Hu, X. L.; Brunschwig, B. S.; Peters, J. C. *J. Am. Chem. Soc.* **2007**, *129*, 8988.
(5) Baffert, C.; Artero, V.; Fontecave, M. *Inorg. Chem.* **2007**, *46*, 1817.
(6) Razavet, M.; Artero, V.; Fontecave, M. *Inorg. Chem.* **2005**, *44*, 4786.
(7) McCrory, C. C. L.; Uyeda, C.; Peters, J. C. *J. Am. Chem. Soc.* **2012**, *134*, 3164.
(8) Wiese, S.; Kilgore, U. J.; DuBois, D. L.; Bullock, R. M. *ACS Catal.* **2012**, *2*, 720.
(9) Kilgore, U. J.; Roberts, J. A. S.; Pool, D. H.; Appel, A. M.; Stewart, M. P.; Rakowski DuBois, M.; Dougherty, W. G.; Kassel, W. S.; Bullock, R. M.; DuBois, D. L. *J. Am. Chem. Soc.* **2011**, *133*, 5861.
(10) Helm, M. L.; Stewart, M. P.; Bullock, R. M.; Rakowski DuBois, M.; DuBois, D. L. *Science* **2011**, *333*, 863.
(11) McNamara, W. R.; Han, Z.; Yin, C.-J.; Brennessel, W. W.; Holland, P. L.; Eisenberg, R. *Proc. Natl. Acad. Sci. U.S.A.* **2012**, *109*, 15594.
(12) McNamara, W. R.; Han, Z.; Alperin, P. J.; Brennessel, W. W.; Holland, P. L.; Eisenberg, R. *J. Am. Chem. Soc.* **2011**, *133*, 15368.
(13) Artero, V.; Chavarot-Kerlidou, M.; Fontecave, M. *Angew. Chem., Int. Ed.* **2011**, *50*, 7238.

(14) Fukuzumi, S.; Yamada, Y.; Suenobu, T.; Ohkubo, K.; Kotani, H. *Energy Environ. Sci.* **2011**, *4*, 2754.
(15) McKone, J. R.; Marinescu, S. C.; Brunschwig, B. S.; Winkler, J. R.; Gray, H. B. *Chem. Sci.* **2014**, *5*, 865.
(16) Uyeda, C.; Peters, J. C. *Chem. Sci.* **2013**, *4*, 157.
(17) *Dithiolene Chemistry: Synthesis, Properties, and Applications*; Stiefel, E. I., Ed.; Wiley: New York, 2003; Progress in Inorganic Chemistry, Vol. *52*.
(18) Sproules, S.; Wieghardt, K. *Coord. Chem. Rev.* **2011**, *255*, 837.
(19) Eisenberg, R.; Gray, H. B. *Inorg. Chem.* **2011**, *50*, 9741.
(20) Zarkadoulas, A.; Koutsouri, E.; Mitsopoulou, C. A. *Coord. Chem. Rev.* **2012**, *256*, 2424.
(21) Das, A.; Han, Z.; Haghighi, M. G.; Eisenberg, R. *Proc. Natl. Acad. Sci. U.S.A.* **2013**, *110*, 16716.
(22) Schrauzer, G. N.; Mayweg, V.; Finck, H. W.; Heinrich, W. *J. Am. Chem. Soc.* **1966**, *88*, 4604.
(23) McCleverty, J. A.; Ratcliff, B. *J. Chem. Soc. A* **1970**, 1631.
(24) Yu, R.; Arumugam, K.; Manepalli, A.; Tran, Y.; Schmehl, R.; Jacobsen, H.; Donahue, J. P. *Inorg. Chem.* **2007**, *46*, 5131.
(25) Solis, B. H.; Hammes-Schiffer, S. *J. Am. Chem. Soc.* **2012**, *134*, 15253.
(26) Baker-Hawkes, M. J.; Billig, E.; Gray, H. B. *J. Am. Chem. Soc.* **1966**, *88*, 4870.
(27) Williams, R.; Billig, E.; Waters, J. H.; Gray, H. B. *J. Am. Chem. Soc.* **1966**, *88*, 43.
(28) Ray, K.; Petrenko, T.; Wieghardt, K.; Neese, F. *Dalton Trans.* **2007**, 1552.
(29) Ray, K.; Begum, A.; Weyhermüller, T.; Piligkos, S.; van Slageren, J.; Neese, F.; Wieghardt, K. *J. Am. Chem. Soc.* **2005**, *127*, 4403.
(30) Petrenko, T.; Ray, K.; Wieghardt, K. E.; Neese, F. *J. Am. Chem. Soc.* **2006**, *128*, 4422.
(31) Ray, K.; DeBeer George, S.; Solomon, E. I.; Wieghardt, K.; Neese, F. *Chem.—Eur. J.* **2007**, *13*, 2783.
(32) Benedito, F. L; Petrenko, T.; Bill, E.; Weyhermüller, T.; Wieghardt, K. *Inorg. Chem.* **2009**, *48*, 10913.
(33) Waters, T.; Wang, X.-B.; Woo, H.-K.; Wang, L.-S. *Inorg. Chem.* **2006**, *45*, 5841.
(34) Note that for these complexes with delocalized bonding between the metal and its ligands, a number of contributing resonance forms may be used to describe the structures. Thus, the cobalt-diaryldithiolene complexes discussed here are arbitrarily depicted in Co(II)-based resonance forms.
(35) Arumugam, K.; Bollinger, J. E.; Fink, M.; Donahue, J. P. *Inorg. Chem.* **2007**, *46*, 3283.
(36) Duan, X.-F.; Feng, J.-X.; Zi, G.-F.; Zhang, Z.-B. *Synthesis* **2009**, 277.
(37) Moorthy, J. N.; Singhal, N.; Senapati, K. *Org. Biomol. Chem.* **2007**, *5*, 767.
(38) Hansch, C.; Leo, A.; Taft, R. W. *Chem. Rev.* **1991**, *91*, 165.
(39) Patra, A. K.; Bill, E.; Bothe, E.; Chlopek, K.; Neese, F.; Weyhermueller, T.; Stobie, K.; Ward, M. D.; McCleverty, J. A.; Wieghardt, K. *Inorg. Chem.* **2006**, *45*, 7877.
(40) Balch, A. L.; Dance, I. G.; Holm, R. H. *J. Am. Chem. Soc.* **1968**, *90*, 1139.
(41) Davison, A.; Howe, D. V.; Shawl, E. T. *Inorg. Chem.* **1967**, *6*, 458.
(42) Felton, G. A. N.; Glass, R. S.; Lichtenberger, D. L.; Evans, D. H. *Inorg. Chem.* **2006**, *45*, 9181.
(43) Connelly, N. G.; McCleverty, J. A.; Winscom, C. J. *Nature* **1967**, *216*, 999.
(44) McCleverty, J. A.; Atherton, N. M.; Connelly, N. G.; Winscom, C. J. *J. Chem. Soc. A* **1969**, 2242.
(45) Dance, I. G.; Miller, T. R. *Inorg. Chem.* **1974**, *13*, 525.
(46) Izutsu, K. *Acid-Base Dissociation Constants in Dipolar Aprotic Solvents*; Blackwell Scientific Publications: Oxford, U.K., 1990; Vol. *35*.
(47) Wiese, S.; Kilgore, U. J.; Ho, M.-H.; Raugei, S.; DuBois, D. L.; Bullock, R. M.; Helm, M. L. *ACS Catal.* **2013**, *3*, 2527.
(48) Crabtree, R. H. *Chem. Rev.* **2012**, *112*, 1536.
(49) Artero, V.; Fontecave, M. *Chem. Soc. Rev.* **2013**, *42*, 2338.
(50) Berben, L. A.; Peters, J. C. *Chem. Commun.* **2010**, *46*, 398.
(51) El, G. S.; Fournier, M.; Cherdo, S.; Guillot, R.; Charlot, M.-F.; Anxolabehere-Mallart, E.; Robert, M.; Aukauloo, A. *J. Phys. Chem. C* **2013**, *117*, 17073.
(52) Cobo, C.; Heidkamp, J.; Jacques, P.-A.; Fize, J.; Fourmond, V.; Guetaz, L.; Jousselme, B.; Ivanova, V.; Dau, H.; Palacin, S.; Fontecave, M; Artero, V. *Nat. Mater.* **2012**, *11*, 802.
(53) Eckenhoff, W. T.; McNamara, W. R.; Du, P.; Eisenberg, R. *Biochim. Biophys. Acta, Bioenerg.* **2013**, *1827*, 958.
(54) Marinescu, S. C.; Winkler, J. R.; Gray, H. B. *Proc. Natl. Acad. Sci. U.S.A.* **2012**, *109*, 15127.
(55) Du, P.; Schneider, J.; Luo, G.; Brennessel, W. W.; Eisenberg, R. *Inorg. Chem.* **2009**, *48*, 4952.
(56) Dempsey, J. L.; Winkler, J. R.; Gray, H. B. *J. Am. Chem. Soc.* **2010**, *132*, 16774.
(57) Valdez, C. N.; Dempsey, J. L.; Brunschwig, B. S.; Winkler, J. R.; Gray, H. B. *Proc. Natl. Acad. Sci. U.S.A.* **2012**, *109*, 15589.
(58) Muckerman, J. T.; Fujita, E. *Chem. Commun.* **2011**, *47*, 12456.
(59) Solis, B. H.; Hammes-Schiffer, S. *Inorg. Chem.* **2011**, *50*, 11252.
(60) Sellmann, D.; Geck, M.; Moll, M. *J. Am. Chem. Soc.* **1991**, *113*, 5259.
(61) Cerdeira, A. C.; Afonso, M. L.; Santos, I. C.; Pereira, L. C. J.; Coutinho, J. T.; Rabaca, S.; Simao, D.; Henriques, R. T.; Almeida, M. *Polyhedron* **2012**, *44*, 228.
(62) Wright, R. J.; Zhang, W.; Yang, X.; Fasulo, M.; Tilley, T. D. *Dalton Trans.* **2012**, *41*, 73.
(63) Bartucz, T. Y.; Golombek, A.; Lough, A. J.; Maltby, P. A.; Morris, R. H.; Ramachandran, R.; Schlaf, M. *Inorg. Chem.* **1998**, *37*, 1555.
(64) Zaffaroni, R.; Rauchfuss, T. B.; Gray, D. L.; De, G. L.; Zampella, G. *J. Am. Chem. Soc.* **2012**, *134*, 19260.
(65) Weber, K.; Kraemer, T.; Shafaat, H. S.; Weyhermueller, T.; Bill, E.; van, G. M.; Neese, F.; Lubitz, W. *J. Am. Chem. Soc.* **2012**, *134*, 20745.
(66) Anslyn, E. V.; Dougherty, D. A. *Modern Physical Organic Chemistry*; University Science Books: Herendon, VA, 2006.
(67) Alves, H.; Simão, D.; Cordeiro Santos, I.; Gama, V.; Teives Henriques, R.; Novais, H.; Almeida, M. *Eur. J. Inorg. Chem.* **2004**, 1318.
(68) Jacques, P.-A.; Artero, V.; Pécaut, J.; Fontecave, M. *Proc. Natl. Acad. Sci. U.S.A.* **2009**, *106*, 20627.
(69) Wiedner, E. S.; Roberts, J. A. S.; Dougherty, W. G.; Kassel, W. S.; DuBois, D. L.; Bullock, R. M. *Inorg. Chem.* **2013**, *52*, 9975.
(70) Plumb, J. B.; Harper, D. J. *Chem. Eng. News* **1990**, *68*, 3.
(71) Bergbreiter, D. E.; Killough, J. M. *J. Am. Chem. Soc.* **1978**, *100*, 2126.
(72) Frigerio, M.; Santagostino, M.; Sputore, S. *J. Org. Chem.* **1999**, *64*, 4537.
(73) Evans, D. F. *J. Chem. Soc.* **1959**, 2003.
(74) *APEX2, v. 2009*; Bruker Analytical X-Ray Systems, Inc.: Madison, WI, 2009.
(75) Sheldrick, G. M. *SADABS, Version 2.03*; Bruker Analytical X-ray Systems, Inc.: Madison, WI, 2000.
(76) Dolomanov, O. V.; Bourhis, L. J.; Gildea, R. J.; Howard, J. A. K.; Puschmann, H. *J. Appl. Crystallogr.* **2009**, *42*, 339.
(77) Connelly, N. G.; Geiger, W. E. *Chem. Rev.* **1996**, *96*, 877.
(78) Shao, Y.; Molnar, L. F.; Jung, Y.; Kussmann, J.; Ochsenfeld, C.; Brown, S. T.; Gilbert, A. T. B.; Slipchenko, L. V.; Levchenko, S. V.; O'Neill, D. P.; DiStasio, R. A., Jr.; Lochan, R. C.; Wang, T.; Beran, G. J. O.; Besley, N. A.; Herbert, J. M.; Yeh Lin, C.; Van Voorhis, T.; Hung Chien, S.; Sodt, A.; Steele, R. P.; Rassolov, V. A.; Maslen, P. E.; Korambath, P. P.; Adamson, R. D.; Austin, B.; Baker, J.; Byrd, E. F. C.; Dachsel, H.; Doerksen, R. J.; Dreuw, A.; Dunietz, B. D.; Dutoi, A. D.; Furlani, T. R.; Gwaltney, S. R.; Heyden, A.; Hirata, S.; Hsu, C.-P.; Kedziora, G.; Khalliulin, R. Z.; Klunzinger, P.; Lee, A. M.; Lee, M. S.; Liang, W.; Lotan, I.; Nair, N.; Peters, B.; Proynov, E. I.; Pieniazek, P. A.; Min Rhee, Y.; Ritchie, J.; Rosta, E.; Sherrill, C. D.; Simmonett, A. C.; Subotnik, J. E.; Woodcock, H. L., III; Zhang, W.; Bell, A. T.; Chakraborty, A. K.; Chipman, D. M.; Keil, F. J.; Warshel, A.; Hehre,

W. J.; Schaefer, H. F., III; Kong, J.; Krylov, A. I.; Gill, P. M. W.; Head-Gordon, M. *Phys. Chem. Chem. Phys.* **2006**, *8*, 3172.
(79) Becke, A. D. *Phys. Rev. A* **1988**, *38*, 3098.
(80) Perdew, J. P. *Phys. Rev. B* **1986**, *33*, 8822.
(81) Lee, C.; Yang, W.; Parr, R. G. *Phys. Rev. B* **1988**, *37*, 785.
(82) Becke, A. D. *J. Chem. Phys.* **1993**, *98*, 5648.
(83) Chai, J.-D.; Head-Gordon, M. *J. Chem. Phys.* **2008**, *128*, 084106.
(84) Wachters, A. J. H. *J. Chem. Phys.* **1970**, *52*, 1033.
(85) Bauschlicher, C. W.; Langhoff, S. R.; Partridge, H.; Barnes, L. A. *J. Chem. Phys.* **1989**, *91*, 2399.
(86) Krishnan, R.; Binkley, J. S.; Seeger, R.; Pople, J. A. *J. Chem. Phys.* **1980**, *72*, 650.
(87) Hariharan, P. C.; Pople, J. A. *Theor. Chim. Acta* **1973**, *28*, 213.
(88) Pulay, P. *Chem. Phys. Lett.* **1980**, *73*, 393.
(89) Pulay, P. *J. Comput. Chem.* **1982**, *3*, 556.
(90) Van Voorhis, T.; Head-Gordon, M. *Mol. Phys.* **2002**, *100*, 1713.
(91) Lange, A. W.; Herbert, J. M. *J. Chem. Phys.* **2010**, *133*, 244111.
(92) Lange, A. W.; Herbert, J. M. *Chem. Phys. Lett.* **2011**, *509*, 77.
(93) Grimme, S. *Chem.—Eur. J.* **2012**, *18*, 9955.